Artifact reduction in electrogastrogram based on empirical mode decomposition method

H. Liang[1] **Z. Lin**[2] **R. W. McCallum**[2]

[1]Center for Complex Systems & Brain Sciences, Florida Atlantic University, Boca Raton, Florida, USA
[2]University of Kansas Medical Center, Department of Medicine, Kansas City, Kansas, USA

Abstract—*Severe contamination of the gastric signal in electrogastrogram (EGG) analysus by respiratory, motion, cardiac artifacts, and possible myoelectrical activity from other organs, poses a major challenge to EGG interpretation and analysis. A generally applicable method for removing a variety of artifacts from EGG recordings is proposed based on the empirical mode decomposition (EMD) method. This decomposition technique is adaptive, and appears to be uniquely suitable for nonlinear, non-stationary data analysis. The results show that this method, combined with instantaneous frequency analysis, effectively separate, identify and remove contamination from a wide variety of artifactual sources in EGG recordings.*

Keywords—*Electrogastrogram, Empirical mode decomposition, Artifact reduction, Hilbert transform, Nonstationary.*

Med. Biol. Eng. Comput., 2000, **38**, 35–41

1 Introduction

SINCE THE landmark development of the electrogastrogram (EGG) by ALVAREZ (1922), cutaneous EGG has been used as a non-invasive approach for physiological and pathophysiological studies of the stomach, and as a clinical tool for the evaluation of gastric dysrhythmia (CHEN and MCCALLUM, 1991, 1993a). Ironically, after 70 years of research, severe contamination of the gastric signal in the EGG by respiratory, motion, and cardiac signals and possible myoelectrical activity from other organs remains a serious problem for EGG interpretation and analysis. This means that without appropriate artifact/noise reduction an EGG evaluation is almost impossible.

The electrical activity of the healthy stomach is mainly composed of rhythmic slow waves and spikes. The fundamental frequency of the gastric signal is ~ 3 cycles/min (3 cpm or 0.05 Hz) in healthy humans, but its waveform is not sinusoidal. This means that the gastric signal may have harmonics. Like the electrocardiogram (ECG), an EGG recording may consist of not only normal rhythms but also dysrhythmia, including tachygastria, bradygastria and arrhythmia. In addition, the amplitude and frequency of the gastric signal component change from time to time (CHEN and MCCALLUM, 1993b). The frequencies of the ECG and respiratory artifact are about 1 Hz and 0.2–0.4 Hz, respectively. A frequency-domain filter could be used to suppress the noise while preserving the gastric signal. This standard approach can be only as effective as the Fourier basis capable to separate signals from noise, which is not the case for broadband signals, e.g. motion artifacts. Moreover, since an electrical signal from the stomach is not sinusoidal, conventional frequency-domain filtering may distort waveforms of the gastric signal by filtering out harmonics of the fundamental frequency of the gastric signal. Artifacts contaminated in EGG cannot therefore be eliminated by using conventional frequency filtering without affecting the gastric signal.

An adaptive filtering technique (CHEN and LIN, 1994) has been shown to improve the quality of extracting relevant information from the EGG. An inherent weakness of this method, however, is that it requires a reference signal that is the comprehensive signal of the various artifacts to be removed. Obviously, it is difficult and sometimes unrealistic to obtain such a reference signal in practical applications, because artifacts are variable, and their nature of distribution is unknown.

An attractive method (LIANG *et al.*, 1997) using feature analysis and neural networks has been reported to realise automatic detection and elimination of motion artifacts in EGG recordings. In this method, once an EGG segment is detected as containing motion artifacts, the whole segment is deleted. However, if there are only limited data available or the motion artifacts occur too frequently, the amount of data lost to artifact rejection may be unacceptable.

We present here a generally applicable method for isolating, identifying and removing a wide variety of artifacts in the EGG using a newly developed method – empirical mode decomposition (EMD) (HUANG *et al.*, 1998*a*). This technique, combined with the Hilbert transform, is ideally suited to nonlinear and non-stationary data analysis. In this paper, we analyse EGG data to demonstrate the effectiveness of this method.

2 Methods

2.1 *Empirical mode decomposition method*

The EMD method was initially proposed in the study of fluid mechanics (HUANG *et al.*, 1998*a*), and found immediate

Correspondence should be addressed to Dr H. Liang; e-mail: liang@walt.ccs.fau.edu

First received 23 July 1999 and in final form 11 October 1999

applications in biomedical engineering (HUANG *et al.*, 1998*b*). The central idea of this method is the sifting process to decompose any given signal into its fundamental modes, those basic building blocks that make up complicated data. If we were to apply a Fourier decomposition to the signal, then the basis functions would be linear combinations of sine and cosine waves, which would be the case if the signal were linear. Fourier analysis therefore merely works well for strictly linear, stationary random functions of time. With the EMD approach, the basic functions are themselves nonlinear functions that can be extracted directly from the data. In other words, an adaptive basis known as the intrinsic mode function (IMF) can be used.

A signal must satisfy two criteria to be an IMF, the first one being that the number of local maxima and the number of local minima differ by at the most one, and the second one being that the mean of its upper and lower envelopes equals zero.

Given these two definitive requirements of an IMF, the problem of interest is how we derive an IMF from a given item of data $X(t)$, e.g. EGG recording, as shown in Fig. 1*a* by a thin solid line. The solution essentially consists of three major steps.

Step (i): Two smooth splines connecting all the maxima and minima of $X(t)$ are constructed to obtain its upper envelope, $X_{up}(t)$ and its lower envelope, $X_{low}(t)$, which are plotted as dotted lines in Fig. 1*a*; The extrema can be simply found by differentiating the data sampled at discrete points and then determining where the sign flips. Once the extrema are identified, all the maxima are connected by a cubic spline line as the upper envelope. The procedure is repeated for the local minima to produce the lower envelope. The upper and lower envelopes should cover all the data between them.

Step (ii): The mean of these two envelopes is subtracted from the data to obtain their difference $X_1(t)$,

$$X_1(t) = X(t) - (X_{up} + X_{low})/2 \tag{1}$$

In Fig. 1*a*, the mean of the envelopes is plotted as a thick solid line.

Step (iii): Steps (i) and (ii) are repeated for $X_1(t)$ until the resulting signal meets the the criteria of an intrinsic mode.

These three steps give the general scenario of the sifting process. It can be seen that the signal $X_1(t)$, as shown in Fig. 1*b* as a thin solid line, is not an IMF, for there are a few negative local maxima and positive minima. This situation is improved by two more interactions, as shown in Fig. 1*c*, although the mean is still not zero. Keep iterating, the convergent signal denoted as $C_1(t)$, Fig. 1*d*, is the first IMF of data $X(t)$, which has a zero local mean.

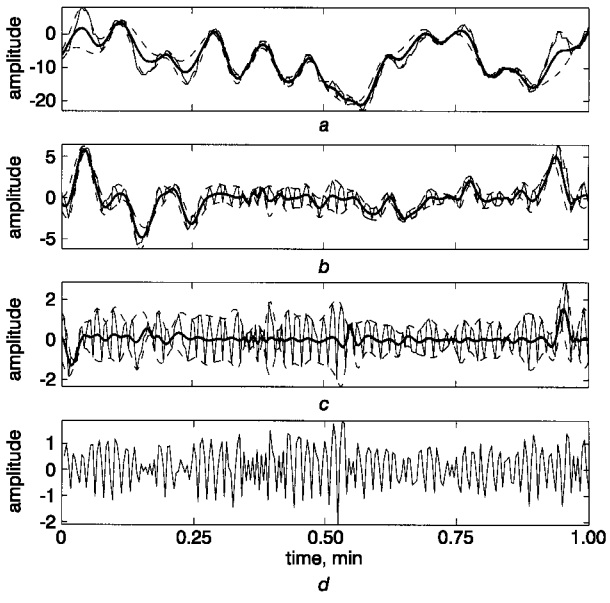

Fig. 1 *Illustration of sifting processes: (a) (——) original data; (– – –) upper and lower envelopes: (——) mean; (b) difference $X_1(t)$, envelopes of maxima and minima and their mean; (c) results shown after two iterations; (d) final IMF*

The residue $R_1(t) = X(t) - C_1(t)$ is then treated as new data subject to the sifting process as described above, yielding the second IMF from $R_1(t)$. The procedure continues until finally a mode becomes less than a predetermined small number or the residue becomes non-oscillatory. The original signal X(t) can thus be expressed as follows:

$$X(t) = \sum_{j=1}^{N} C_j(t) + R_N(t) \tag{2}$$

where N is the number of IMFs, $R_N(t)$ is the final residue, which can be either the mean trend or a constant, and functions $C_j(t)$ are nearly orthogonal to each other, and all have zero means. By the nature of the decomposition procedure, the technique decomposes data into N fundamental components, each with a distinct time scale. More specifically, the first component has the smallest time scale, which corresponds to the fastest time variation of data. As the decomposition process proceeds, the time scale increases, and hence the mean frequency of the mode decreases. Since the decomposition is based on the local characteristic time scale of the data to yield an adaptive basis, it is applicable to nonlinear and non-stationary data in general and to EGG data in particular, as considered in the following section.

2.2 *Hilbert transform*

Once all the IMFs are found, the instantaneous frequency of each component can be readily obtained by utilising the Hilbert transform, which can be used later for signal identification.

The Hilbert transform has been widely used in order to obtain the analytic signal associated with the real signal $x(t)$, and, consequently, its instantaneous envelope and phase functions. The instantaneous frequency, which is of interest here, can be further derived from the instantaneous phase, and its definition is given below (OPPENHEIM and SCHAFER, 1975).

Given a time series $x(t)$, the corresponding analytic signal is defined as

$$z(t) = x(t) + iH[x(t)] = a(t)\exp[i\theta(t)] \tag{3}$$

where $a(t)$ and $\theta(t)$ are the instantaneous amplitude and phase of the analytic signal $z(t)$, and the imaginary part $H[x(t)]$ is the Hilbert transform of $x(t)$:

$$H[x(t)] = \mathcal{P}\left[\frac{1}{\pi}\int_{-\infty}^{\infty}\frac{x(u)}{t-u}du\right]$$

Here, the notion $\mathcal{P}$ indicates the Cauchy principal value of the integral (OPPENHEIM and SCHAFER, 1975). If $\mathcal{F}\{x(t)\}$ and $\mathcal{F}\{z(t)\}$ are respectively the Fourier transforms of $x(t)$ and $z(t)$, the above relationship is expressed in the frequency domain by

$$\mathcal{F}\{z(t)\} = \begin{cases} 2\mathcal{F}\{x(t)\} & \text{if} \quad \omega > 0 \\ \mathcal{F}\{x(t)\} & \text{if} \quad \omega = 0 \\ 0 & \text{if} \quad \omega < 0 \end{cases} \tag{4}$$

Thus, the analytic signal, which still retains the information content of its original real signal, can be obtained from eqn 4. With the instantaneous phase, it is then possible to define in a unique way the concept of instantaneous frequency by

$$\omega(t) = d\theta(t)/dt \tag{5}$$

By virtue of the analytic signal, the given signal can be faithfully represented by the amplitude and frequency as

functions of time in a three-dimensional plot, in which the amplitude distribution on the time-frequency plane is referred to as the Hilbert spectrum.

3 Experimental results

The artifact reduction procedure consists of three major steps. The first step is to decompose the data into a number of IMF components by empirical mode decomposition. The second step is to perform the Hilbert transform to each of the IMF components to obtain its instantaneous frequency. The final step is to identify the artifactual or relevant signals on the basis of prior knowledge and then extract the cleaner EGG.

A validation study is first performed to test the efficiency and performance of the artifact reduction method. Two sets of EGG data, each from a different subject, are then selected to illustrate the application procedure of the EMD method. Followed is the extraction of gastric slow waves using this method from an EGG recording with motion interference.

3.1 *Validation*

Computer simulations were conducted to evaluate the performance of the proposed artifact reduction method. The simulated EGG signal (Fig. 2*c*) was composed of a pure gastric electrical signal (Fig. 2*a*), respiratory and motion artifacts (Fig. 2*b*) and white noise. The pure gastric electrical signal was obtained from a pair of serosal electrodes in a patient. The respiratory and moton artifacts were obtained using a pneumatrace belt. The EMD method yielded eight IMF components as shown in Fig. 3. The instantaneous frequencies of these IMF components obtained using the Hilbert transform are given in Fig. 4, in which the third and second components are the gastric signal and its harmonic, thus indicating that the first component is likely to be the respiratory artifact. The extracted gastric signal (components 2 and 3) is shown in Fig. 2*d*. For comparison, the result of band-pass filtering with low and high cut-off frequencies of 0.5 and 6 cpm, respectively, is shown in Fig. 2*e*. It is evident from Fig. 2 that the EMD method produces a superior result. This can be clearly seen by examining the Fourier spectra shown in Fig. 5, in which the spectra of the mixed signal, the pure gastric signal, the gastric signal extracted using the EMD method and that obtained using conventional band-pass filtering are shown in dashed, dotted, thick solid and thin solid lines, respectively. It can be seen from these curves that the spectrum of the gastric signal extracted using the EMD method is slightly different to that of the pure gastric signal, whereas conventional band-pass filtering results in a large deviation, particularly at high frequencies.

To quantify the performance of the EMD method, the following relative error is defined:

$$\delta = \frac{\sum_f [P(f) - P'(f)]^2}{\sum_f P^2(f)}$$

where $P(f)$ is the spectral density of the pure gastric signal, $P'(f)$ is the spectral density of the extracted or filtered gastric signal, and f ranges from 0.5 to 9 cpm. Indeed, the EMD

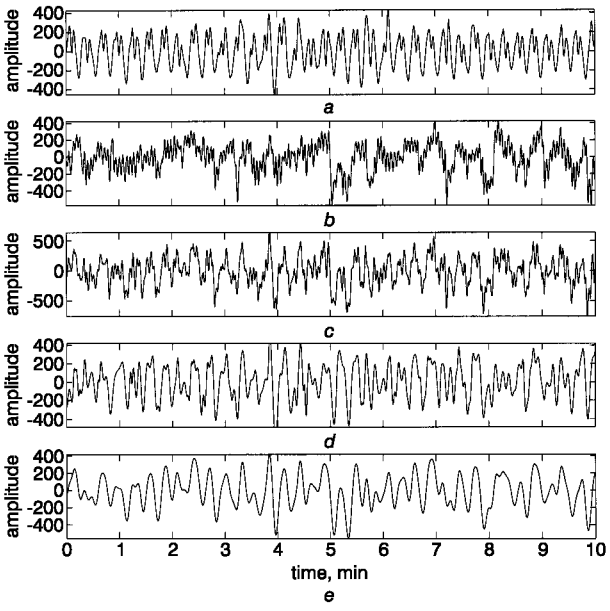

Fig. 2 *Signals used in simulation and extracted clean EGGs using EMD method and conventional band-pass filtering: (a) pure gastric signal obtained from serosal electrodes in patient; (b) respiratory and motion artifact; (c) simulated EGG: mixture of signal in (a) and (b), together with white noise; (d) extracted clean EGG using EMD method; (e) extracted EGG using band-pass filtering*

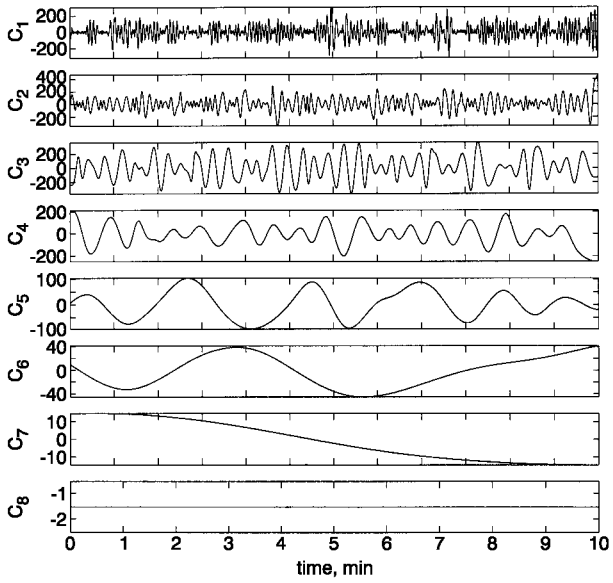

Fig. 3 *Eight IMF components of simulated EGG in Fig. 2c obtained by EMD method*

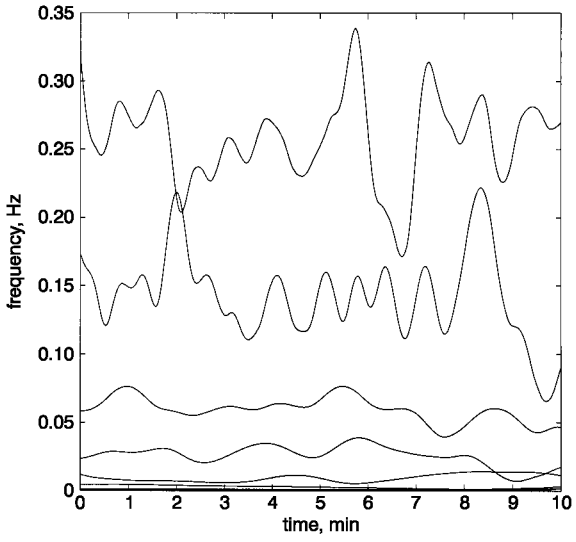

Fig. 4 *Instantaneous frequencies of IMF components in Fig. 3*

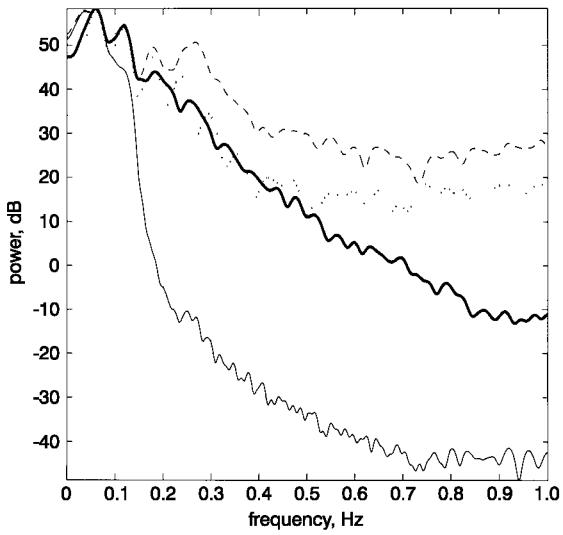

Fig. 5 *Comparison of power spectra of mixed signal (– – –), pure gastric signal (· · ·), extracted gastric signal using EMD method (——) and that obtained using conventional bandpass filtering (——)*

method yields a smaller relative error (0.0595) than that of conventional bandpass filtering (0.151).

3.2 *Applications to EGG recording*

The EGG data used in this study were obtained from both healthy subjects and patients with dyspeptic symptoms by using a portable EGG recorder* with low and high cut-off frequencies of 1.0 and 18.0 cpm, respectively. Three silver/silver chloride electrodes† were placed on the abdominal skin over the stomach. Two epigastric electrodes were connected to yield a bipolar EGG signal, one electrode at the midpoint between the xiphoid and the navel, and the other 5 cm to the left and 5 cm above this point. The third electrode, placed at the left costal margin horizontal to the first electrode, was

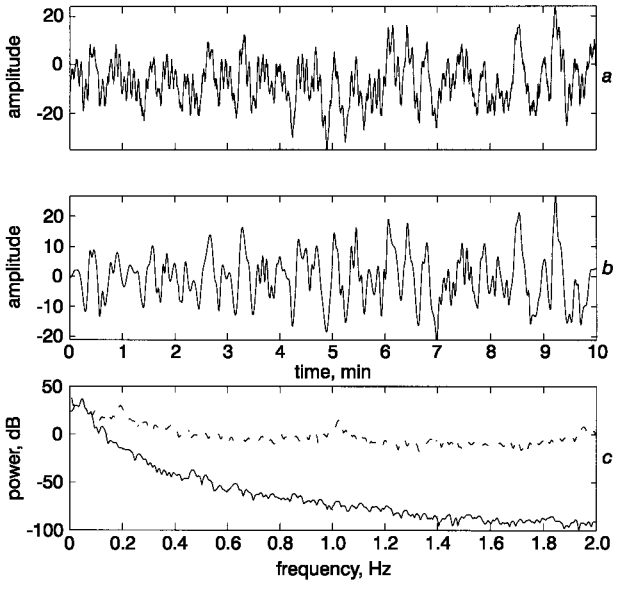

Fig. 6 *Typical EGG recording from one healthy subject before and after artifact reduction and power spectra: (a) original signal; (b) extracted clean EGG; (c) power spectra of signals in (a) (– · – ·) and (b) (——)*

*Synectics, Irving, TX

†VER MED, Bellow Falls, VT

used as a reference. The signal was digitised on-line at a sampling frequency of 1 Hz.

In the first application, a 10-min EGG recording from a healthy subject, as shown in Fig. 6*a*, was used in the experiment. Fig. 7 shows the resulting IMF components. The Hilbert transforms of these IMF components give their instantaneous frequencies shown in Fig. 8. The first three components correspond to the heartbeat, respiratory artifact and harmonic signal, respectively. Component 4 is assumed to be the ongoing gastric slow wave around 3 cpm, which clearly reflects the non-stationary nature of gastric activity.

This can be further confirmed by scrutinising the frequency content of each component, as shown in Fig. 9. The peak frequencies of components 1, 2, 3 and 4 are successively 1.02 Hz, 0.2 Hz, 0.1 Hz and 0.05 Hz, which correspond to the heartbeat, respiratory artifact, harmonic signal and gastric slow wave, respectively. For comparison, the extracted gastric signal (components 3 and 4) is plotted in Fig. 6*b*. The frequency contents of the original EGG and extracted gastric signal are shown in Fig. 6*c*. It can be seen from these figures that the

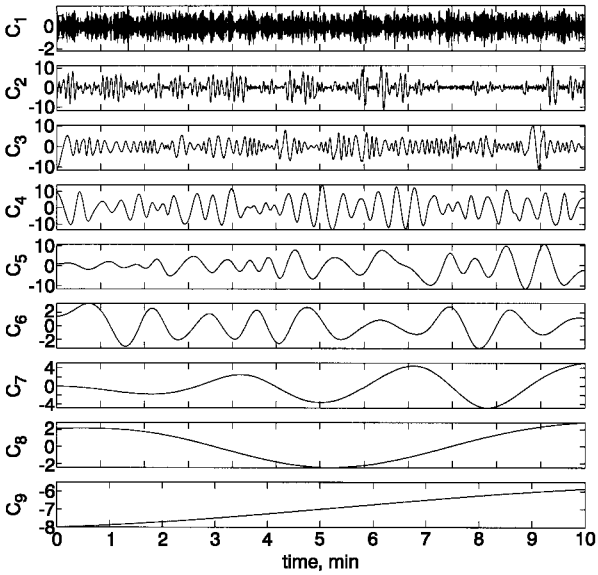

Fig. 7 *IMF components from EGG data in Fig. 6*a

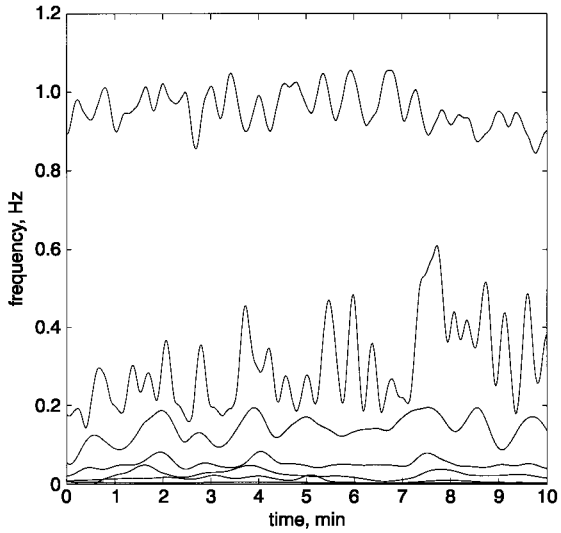

Fig. 8 *Instantaneous frequencies of IMF components in Fig. 7. There is considerable frequency variation, an indication that the EGG is not stationary*

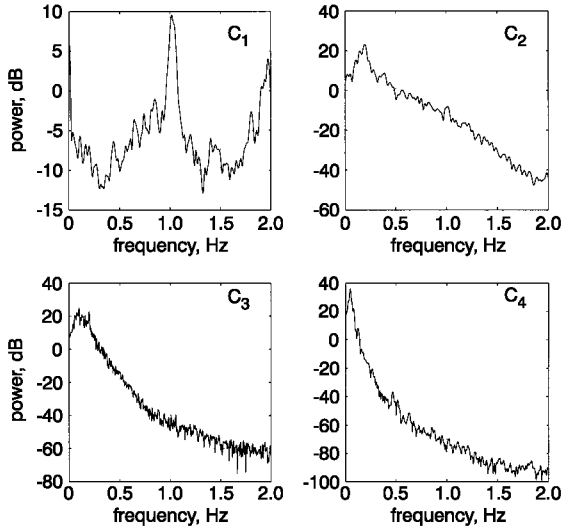

Fig. 9 *The power spectra of the first four IMF components, where the peak frequency in each subplot is, respectively, 1.02 Hz, 0.2 Hz, 0.1 Hz and 0.05 Hz. These frequencies respectively correspond to the heartbeat, respiratory artifact, harmonic signal and gastric slow wave*

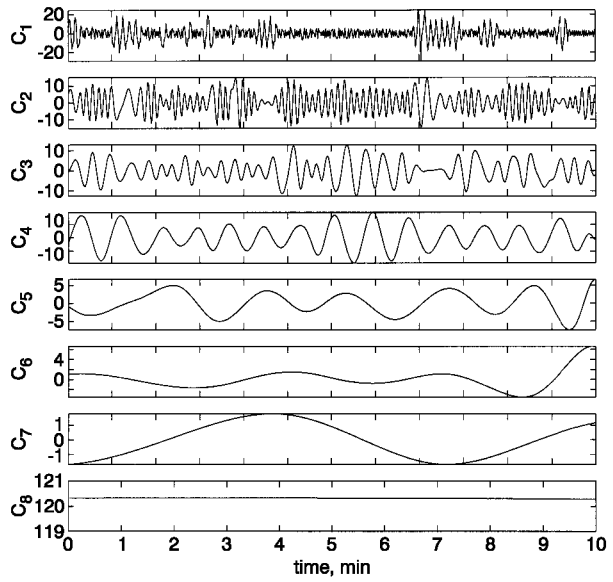

Fig. 11 *Resulting empirical mode decomposition components from EGG signal in Fig. 10a. Notice the last component, C_8, is not an IMF; it is the trend*

gastric signal component is effectively extracted whereas other noise and artifacts are greatly reduced.

In the second application, an EGG recording from a patient with dyspeptic symptoms was used. Fig. 10*a* shows a 10-min EGG signal. These data, when subjected to the empirical mode decomposition method, yielded seven components and a residue, as shown in Fig. 11. The residue obviously should be the DC component or the trend in the data, which is a further benefit of the EMD method. The instantaneous frequencies of the IMF components are shown in Fig. 12, in which the frequency of the first two components fluctuating over a considerable range at 0.14 Hz corresponds to the respiratory artifact. The resulting signal in the time domain after the first two IMF components and the DC component have been removed is shown in Fig. 10*b*. The Fourier spectra of the extracted and orginal signals are shown in Fig. 10*c*, from which it can be seen that both the high-frequency and DC components are effectively reduced. The remaining signals are dominated by bradygastria, with a frequency of 1.5 cpm.

To further illustrate the effectiveness of the EMD method, a 10-min EGG recording with heavy motion interference, which is a more difficult artifact to remove, was selected. In contrast to the aforesaid examples, it can be seen from the EGG recording as shown in Fig. 13*a*, that the weak gastric signal is mostly submerged in the motion artifacts. It is therefore necessary to firstly use a proper preprocessing method to weaken the power of the motion interference, and to then apply the EMD method. To tackle this difficult problem, a preprocessing procedure was devised that placed a threshold on the raw EGG data $x(t)$ according to the following formula:

$$x(t) = \begin{cases} p1 & \text{if} \quad x(t) > p1 \\ p2 & \text{if} \quad x(t) < p2 \\ x(t) & \text{others} \end{cases}$$

where $p1$, $p2$, the applied thresholds as plotted in Fig. 13*a* as

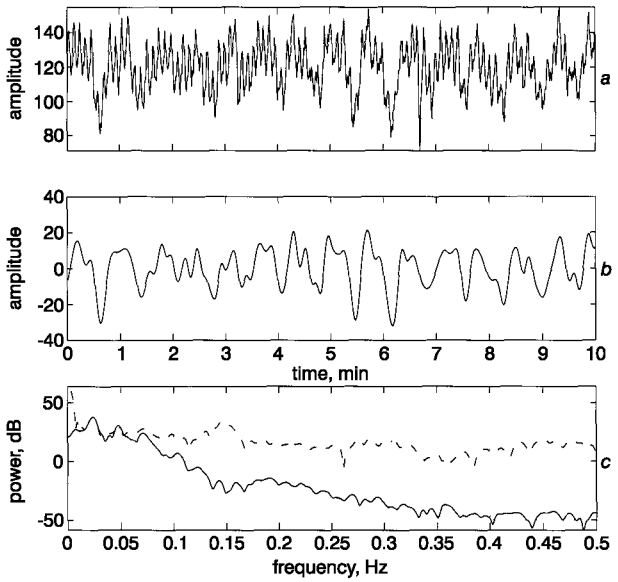

Fig. 10 *EGG recording measured from patient with dyspeptic symptoms before and after artifact reduction and power spectra: (a) original signal; (b) extracted clean EGG after removing first two IMFs and DC component; (c) power spectrum of clean EGG (——) in comparison with that of the original signal (– · – · –)*

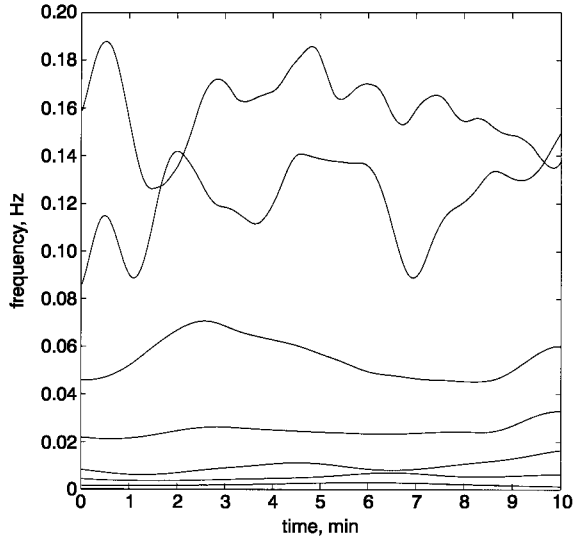

Fig. 12 *Instantaneous frequencies of IMF components in Fig. 11*

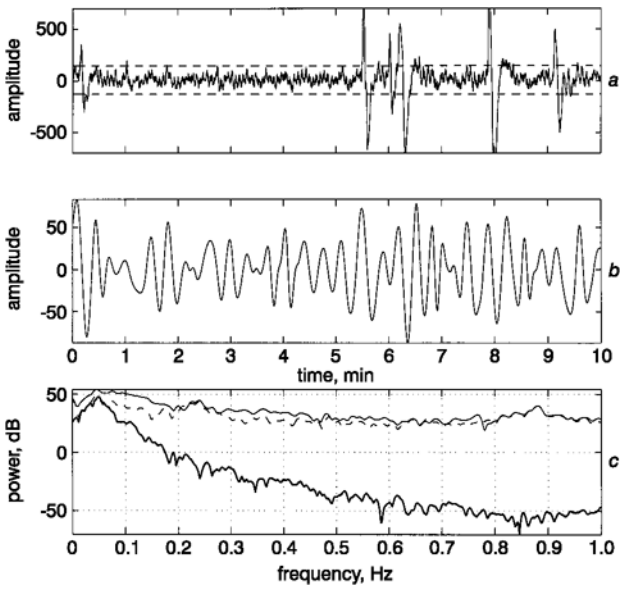

Fig. 13 *EGG recording with motion artifacts before and after artifact reduction and power spectra: (a) original EGG recording; (– – –) applied thresholds; values exceeding these limits are discorded; (b) extracted clean EGG after removing first two IMFs and DC component; (c) power spectrum of clean EGG (——) in comparison with those of original EGG data (——) and preprocessed data (– – –). where the fact that the difference between the latter two is almost indiscernible implies that the gastric signal embedded in the EGG is not affected or affected to a lesser extent by our preprocessing procedure*

dashed lines, are, respectively, the mean $\pm 3 \times$(standard deviation) of the EGG segment without severe motion artifacts. By comparing the power spectra before (thin solid line) and after (dotted lines) thresholding of the EGG data, as shown in Fig. 13*c*, it can be seen that the power of the EGG data is not affected or affected to a lesser extent. A more sophisticated preprocessing method can of course be used that applies the adaptive thresholding approach (DONOHO and JOHNSTONE, 1995). However, we found this method is adequate for our purpose.

Following use of the empirical mode decomposition and signal identification procedure as stated above, the IMF components of the preprocessed EGG are presented in Fig. 14. The extracted gastric signal (component 4) is shown in Fig. 13*b*, and its power spectrum is plotted in Fig. 13*c* as a thick solid line. It is clearly observed that the motion artifacts and high-frequency components in the EGG recording are greatly reduced.

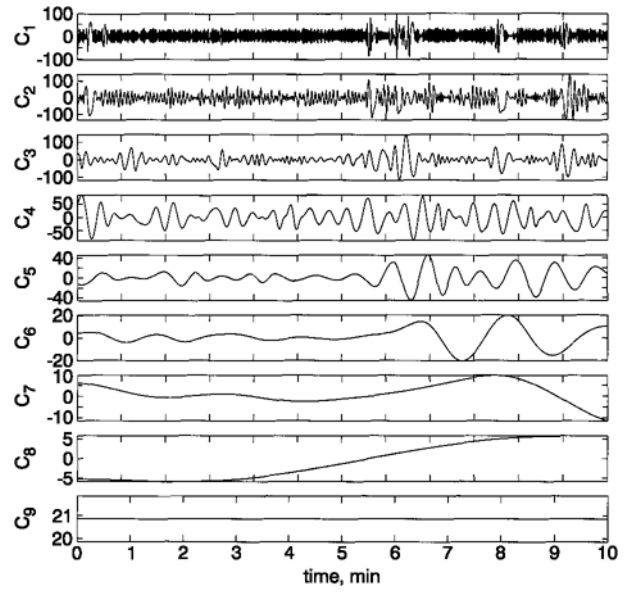

Fig. 14 *Nine IMF components obtained using EMD method*

4 Discussion and conclusions

A newly developed signal processing method (EMD) has been introduced and its successful applications in artifact reduction in cutaneous EGG presented.

EGG is a cutaneous measurement of electrical activity of the stomach. It is very attractive because it is non-invasive and does not disturb the ongoing activities of the stomach. Unlike other surface electrophysiological measurements such as electrocardiography (ECG), however, the clinical applications of this non-invasive method have been limited (CHEN and MCCALLUM, 1993*a*). One of the main problems with the EGG method is the poor quality of the recording, i.e. the weakness of the real gastric signal and the heavy interference from ECG, respiratory and motion artifacts. As a result, direct visual analysis of the EGG is impossible. Several methods have been designed and applied to improve the quality of the EGG, including bandpass filtering (NELSEN and KOHATSU, 1968; STODDARD *et al.*, 1981), fast Fourier transform (BROWN *et al.*, 1975; VAN DER SCHEE and GRASHUIS, 1987), phase-lock filtering (SMALLWOOD, 1978), autoregressive modelling (LINKENS and DATARDINA, 1978), adaptive filtering (CHEN and LIN, 1994) and neural networks (LIANG *et al.* 1997). Although each of these methods has its advantages over the others, they are of only limited use in practical applications. This is because there are some crucial restrictions in all of the above methods: the linearity of the system and stationarity of the data. It has already been proved that the amplitude and frequency of the gastric signal in the EGG may change over time and that these changes are non-stationary (LIN and CHEN, 1994, 1995; CHEN *et al.* 1993*b*). In addition, it has also been shown that an EGG signal has a chaotic behaviour with a strange attractor (LINDBERG, 1996). An advanced method for processing nonlinear and non-stationary signals is therefore needed to improve the quality of the EGG.

The EMD method (HUANG *et al.*, 1998*a*) introduced in this paper decomposes any given data into a finite and often small number of IMFs that admit well-behaved Hilbert transforms. With the EMD approach, the basic functions used to represent the given signal are nonlinear functions that can be extracted directly from the data. In other words, an adaptive basis known as IMF can be used. Since the decomposition is based on the local characteristic time scale of the data to yield the adaptive basis, the EMD method is applicable to nonlinear and non-stationary processes. As stated above, both the gastric signal and artifacts in the EGG may be non-stationary and therefore the EMD method is well suited to processing of the EGG. Another advantage of this method is that the decomposition components usually offer a more physically meaningful interpretation of the underlying dynamic processes. To identify the artifacts and gastric signal in the EGG, the next step is to perform the Hilbert transform on each of the decomposed IMF components to obtain their instantaneous frequencies. Based on prior knowledge of the frequency range of the gastric signal, it is easy to extract the clean gastric signal from the IMF components of the EGG data. Experiments on real EGG data showed that the EMD method does yield more efficient artifact reduction in the EGG while leaving the gastric signal unaffected.

There is much room for improvement in the EMD method. The spline fitting is the essential step in generating the IMF. Although the present envelope-mean method works well in most cases, problems still exist. The cubic spline fitting adopted here has both overshoot and undershoot problems. These problems can be alleviated by using more sophisticated spline methods, such as the higher-order spline program. However, such improvement would probably be marginal. It should be noted that an additional step may have to be taken to preprocessing the EGG data before the EMD method is used if the gastric signal is embedded in stronger motion artifacts. This is because the EMD method is based on the identification of scales from successive extrema (HUANG *et al.*, 1998*a*). If the gastric signals are phase-locked with and occur only at the maximum slope regions of the strong motion artifacts, then it will be difficult to recover the gastric signal. In this case, either a hard-threshold or differentiation of original data could be used before using the EMD method. It is also worth noting that the EMD method uses the data effectively, which is particularly useful where only limited data are available.

In conclusion, this paper has shown that the EMD method combined with instantaneous frequency analysis is powerful and very useful in removing artifacts in cutaneous EGG recording.

References

ALVAREZ, W. C. (1922): 'The electrogastrogram and what it shows', *J. Amer. Med. Assoc.*, **78**, pp. 1116–1118

BROWN, B. H., SMALLWOOD, R. H., Duthie H. L., and STODDARD, C. J. (1975): 'Intestinal smooth muscle electrical potentials recorded from surface electrodes', *Med. & Biol. Eng.*, **13**, pp. 97–103

CHEN, J., MCCALLUM, R. W. (1991): 'Electrogastrogram: Measurement, analysis and prospective applications', *Med. Biol. Eng. Comput.*, **29**, pp. 339–350

CHEN, J. D. Z. and MCCALLUM, R. W. (1993a): 'Clinical application of electrogastrogram', *Am. J. Gastroenterol.*, **88**, pp. 1324–1336

CHEN, J., Stewart, W. R. and MCCALLUM, R. W. (1993*b*): 'Adaptive spectral analysis of episodic rhythmic variations in the cutaneous electrogastrogram', *IEEE Trans.*, **BME-40**, pp. 128–135

CHEN, J., and LIN, Z. Y. (1994): 'Comparison of adaptive filtering in time-, transform- and frequency-domain: An electrogastrographic study', *Ann. Biomed. Eng.*, **22**, pp. 423–431

DONOHO, D., and JOHNSTONE, I. (1995): 'Adapting to unknown smoothness via wavelet shrinkage', *J. Am. Stat. Assoc.*, **90**, pp. 1200–1224

HUANG, N. E., SHEN, Z., LONG, S. R., WU, M. L. C., SHIH, H. H., ZHENG, Q. N., YEN, N. C., TUNG, C. C. and LIU, H. H. (1998*a*): 'The empirical mode decomposition and the Hilbert spectrum for nonlinear and non-stationary time series analysis'. *Proc. Roy. Soc. LOND A MAT*, **454**, pp. 903–995

HUANG, W., Shen, Z., HUANG, N. E. and Fung, Y. C. (1998*b*): 'Engineering analysis of biological variables: an example of blood pressure over 1 day', *Proc. Nat. Acad. Sci. USA*, **95**, pp. 4816–4821

LIANG, J., CHEUNG, J. Y., CHEN, J. D. Z. (1997): 'Detection and deletion of motion artifacts in electrogastrogram using feature analysis and neural networks', *Ann. Biomed. Eng.*, **25**, pp. 850–857

LIN, Z. Y., CHEN, J. (1994): 'Time-Frequency Representation of the Electrogastrogram – application of the exponential distribution', *IEEE Trans.*, **BME-41**, pp. 267–275

LIN, Z. Y., CHEN, J. (1995): 'Comparison of three running spectral analysis methods for electrogastrographic signals', *Med. Biol. Eng. Comput.*, **33**, pp. 596–604

LINDBERG, G. (1996): 'Is the electrogastrogram a chaotic parameter?', *Gastroenetrology*, **110**, pp. A707

LINKENS, D. A. and DATARDINA, S. P. (1978): 'Estimation of frequencies of gastrointestinal electrical rhythms using autoregressive modelling', *Med. & Biol. Eng. & Comput.*, **16**, pp. 262–268

NELSEN, T. S. and KOHATSU, S. (1968): 'Clinical electrogastrography and its relationship to gastric surgery', *Am. J. Surg.*, **116**, pp. 215–222

OPPENHEIM, A. and SCHAFER, R. (1975): 'Digital signal processing' (Prentice-Hall, New-Jersey)

SMALLWOOD, R. H. (1978): 'Analysis of gastric electrical signals from surface electrodes using phase-lock techniques', *Med. & Biol. Eng. & Comput.*, **16**, pp. 507–518

STODDARD, C. J., SMALLWOOD, R. H. and DUTHIE, H. L. (1981): 'Electrical arrhythmias in the human stomach,' *Gut*, **22**, pp. 705–712

VAN DER SCHEE, E. J. and GRASHUIS, J. L. (1987): 'Running spectrum analysis as an aid in the representation and interpretation of electrogastrographic signals', *Med. & Biol. Eng. & Comput.*, **25**, pp. 57–62

Author's biography

HUALOU LIANG received his MSc in electronic engineering from Dalian University of Technology, China, in 1993 and his PhD in physics from the Chinese Academy of Sciences, China, in 1996. Since completing his PhD, he has held three postdoctoral research positions in Tel-Aviv University, Israel, the Max-Planck-Institute for Biological Cybernetics, Germany, and Florida Atlantic University, USA, respectively. He is currently with the Center for Complex Systems and Brain Sciences, Florida Atlantic University, USA. His research interests are mainly cognitive and computational neuroscience, signal processing and its applications in biomedical engineering.